


Subtype-Specific Roles of Ellipsoid Body Ring Neurons in Sleep Regulation in *Drosophila*

Wei Yan (闫薇),¹ Hai Lin (林海),² Junwei Yu (于俊伟),³ Timothy D. Wiggin,³ Litao Wu (伍立桃),¹ Zhiqiang Meng (孟志强),^{1,4,6} Chang Liu (刘畅),^{1,4,5} and  Leslie C. Griffith³

¹Brain Cognition and Brain Disease Institute, Shenzhen Institute of Advanced Technology, Chinese Academy of Sciences, Shenzhen-Hong Kong Institute of Brain Science-Shenzhen Fundamental Research Institutions, Shenzhen, 518000, China, ²Central Research Institute, United Imaging Healthcare, Shanghai, 200032, China, ³Department of Biology, National Center for Behavioral Genomics and Volen Center for Complex Systems, Brandeis University, Waltham, Massachusetts 02453, ⁴CAS Key Laboratory of Brain Connectome and Manipulation, Shenzhen, 518000, China, ⁵Shenzhen Key Laboratory of Viral Vectors for Biomedicine, Shenzhen, 518000, China, and ⁶Shenzhen Key Laboratory of Drug Addiction, Shenzhen, 518000, China

The ellipsoid body (EB) is a major structure of the central complex of the *Drosophila melanogaster* brain. Twenty-two subtypes of EB ring neurons have been identified based on anatomic and morphologic characteristics by light-level microscopy and EM connectomics. A few studies have associated ring neurons with the regulation of sleep homeostasis and structure. However, cell type-specific and population interactions in the regulation of sleep remain unclear. Using an unbiased thermogenetic screen of EB drivers using female flies, we found the following: (1) multiple ring neurons are involved in the modulation of amount of sleep and structure in a synergistic manner; (2) analysis of data for $\Delta P(\text{doze})/\Delta P(\text{wake})$ using a mixed Gaussian model detected 5 clusters of GAL4 drivers which had similar effects on sleep pressure and/or depth: lines driving arousal contained R4m neurons, whereas lines that increased sleep pressure had R3m cells; (3) a GLM analysis correlating ring cell subtype and activity-dependent changes in sleep parameters across all lines identified several cell types significantly associated with specific sleep effects: R3p was daytime sleep-promoting, and R4m was nighttime wake-promoting; and (4) R3d cells present in 5HT7-GAL4 and in GAL4 lines, which exclusively affect sleep structure, were found to contribute to fragmentation of sleep during both day and night. Thus, multiple subtypes of ring neurons distinctively control sleep amount and/or structure. The unique highly interconnected structure of the EB suggests a local-network model worth future investigation; understanding EB subtype interactions may provide insight how sleep circuits in general are structured.

Key words: central complex; *Drosophila melanogaster*; ellipsoid body; ring neurons; sleep; sleep structure

Significance Statement

How multiple brain regions, with many cell types, can coherently regulate sleep remains unclear, but identification of cell type-specific roles can generate opportunities for understanding the principles of integration and cooperation. The ellipsoid body (EB) of the fly brain exhibits a high level of connectivity and functional heterogeneity yet is able to tune multiple behaviors in real-time, including sleep. Leveraging the powerful genetic tools available in *Drosophila* and recent progress in the characterization of the morphology and connectivity of EB ring neurons, we identify several EB subtypes specifically associated with distinct aspects of sleep. Our findings will aid in revealing the rules of coding and integration in the brain.

Received July 10, 2022; revised Sep. 22, 2022; accepted Oct. 26, 2022.

Author contributions: W.Y., J.Y., L.W., Z.M., and C.L. performed research; W.Y., H.L., and T.D.W. analyzed data; W.Y., H.L., and C.L. wrote the first draft of the paper; C.L. and L.C.G. designed research; C.L. and L.C.G. edited the paper.

This work was supported by National Natural Science Foundation of China 32071009 to C.L.; Guangdong Basic and Applied Basic Research Foundation 2020A1515011055 to C.L.; CAS Key Laboratory of Brain Connectome and Manipulation (2019DP173024); Shenzhen Fundamental Research Program JCYJ20210324103014037 to H.L.; and National Institutes of Health Grant R01MH67284 to L.C.G.

The authors declare no competing financial interests.

Correspondence should be addressed to Chang Liu at chang.liu3@siat.ac.cn or Leslie C. Griffith at griffith@brandeis.edu.

<https://doi.org/10.1523/JNEUROSCI.1350-22.2022>

Copyright © 2023 Yan et al.

This is an open-access article distributed under the terms of the Creative Commons Attribution 4.0 International license, which permits unrestricted use, distribution and reproduction in any medium provided that the original work is properly attributed.

Introduction

Sleep plays critical roles in many physiological functions. Sleep regulation in the brain is a complex process modulated at the molecular, cellular, circuit, and network levels (John et al., 2016; Scammell et al., 2017; Bringmann, 2018; Herice and Sakata, 2019; D. Liu and Dan, 2019). Previous studies in *Drosophila melanogaster* have revealed multiple cell types and neural circuits that participate in the regulation of sleep amount, structure, and homeostasis.

The ellipsoid body (EB) contributes to regulation of multiple behaviors, including spatial orientation, navigation, arousal, and sleep (Bausenwein et al., 1994; Lebestky et al., 2009; Ofstad et al.,

2011; Seelig and Jayaraman, 2015; Fisher et al., 2019; Kim et al., 2019; Kottler et al., 2019). As one of the central structures on the midline of the fly brain, the EB receives direct input from, and sends output to, many brain regions. This high level of connectivity positions the EB to be a center for integration of multiple information streams, including visual, motor, mechanosensory, and circadian input, allowing it to functionally tune complex behaviors (Franconville et al., 2018).

The organization within the EB also exhibits complexity. With recent progress on morphology and connectivity of the EB, 22 distinct subtypes of ring neurons have been identified (Hulse et al., 2021). Each subtype of ring neuron typically contains a dendritic arborization lateral to the EB, then projects a single axon into the concentric laminated structure within the EB neuropil. The projections from each subtype of ring neuron form distinct layers within the neuropil, terminating in different rings at specific depths along the anterior-posterior axis where they interconnect (Hanesch et al., 1989; Young and Armstrong, 2010; Lin et al., 2013). These connections, between neurons of the same type, provide each ring neuron's strongest inputs (Isaacman-Beck et al., 2020; Hulse et al., 2021) and suggest a structural basis for local communication and synergism for sleep regulation.

Despite the growing understanding of EB connectivity, specific roles for each subtype of ring neuron in sleep are limited. One subtype of R5 neuron (initially referred to as R2) has been shown to drive a persistent sleep on secession of thermoactivation, suggesting a role in sleep drive and homeostasis (Donlea et al., 2014; S. Liu et al., 2016; Pimentel et al., 2016). Another study showed that single R5 neurons get synchronized by circadian input and the power of slow-wave oscillations in R5 neurons has been associated with increased sleep drive (Raccuglia et al., 2019). 5HT7-GAL4⁺ EB neurons, which consist of several subtypes including R3d, R3p, and R4d and are modulated by serotonergic signaling, can regulate sleep architecture (C. Liu et al., 2019). Despite these important findings, the scope of ring neuron involvement in the regulation of sleep is not clear.

In the present study, we take an unbiased approach, screening 34 drivers that label different combinations of subtypes of ring neurons by thermoactivation using the warmth-sensitive cation channel dTrpA1 (Hamada et al., 2008). Most drivers label multiple ring neurons, and activation of many drivers resulted in significant changes in sleep amount and/or sleep structure. The complexity of the tools and phenotypes necessitated developing computational approaches for assessing the importance of each subtype. Using P(wake) and P(doze) analysis with a mixed Gaussian model, five clusters of drivers were found to regulate sleep depth and pressure during the day and/or at night, respectively. Furthermore, a GLM analysis based on the GAL4 expression pattern and the sleep behavior on 24 h activation suggests several types of ring neuron contribute to sleep regulation consistent with and extending the findings from the Gaussian model. Finally, using genetic suppression of intersected population strategy, we identified a subpopulation of neurons which is sufficient to fragment sleep during both day and night. Although how the ring neurons cooperate to coherently modulate sleep is not yet clear, the identification of roles for specific cell types provides an important piece of the puzzle.

Materials and Methods

Animals. Unless specified, flies were reared on standard cornmeal food (each 1 L H₂O: 70 g cornmeal, 50 g sucrose, 10 g soybean powder,

20 g yeast powder, 6 g agar, and 3 g methyl 4-hydroxybenzoate) at 23°C with 60% relative humidity and under a regimen of 12 h light/12 h dark. Flies were allowed to freely mate after eclosion, and mated females aged 2–5 d were used for all experiments. GAL4 lines: R12B01 (RRID:BDSC_48487), R15B07 (RRID:BDSC_48678), R28D01 (RRID:BDSC_47342), R28E01 (RRID:BDSC_49457), R38B06 (RRID:BDSC_49986), R38G08 (RRID:BDSC_50020), R38H02 (RRID:BDSC_47352), R41A08 (RRID:BDSC_50108), R41F05-GAL4 (RRID:BDSC_50133), R47F07 (RRID:BDSC_50320), R48B10 (RRID:BDSC_50352), R49E12 (RRID:BDSC_38693), R53F11 (RRID:BDSC_50443), R53G11 (RRID:BDSC_69747), R54B05 (RRID:BDSC_69148), R56C09 (RRID:BDSC_39145), R64H04 (RRID:BDSC_39323), R70B04 (RRID:BDSC_39513), R70B05 (RRID:BDSC_47721), R73A06 (RRID:BDSC_39805), R73B05 (RRID:BDSC_48312), R81F01 (RRID:BDSC_40120), R84H09 (RRID:BDSC_47803), Aph^{CS07} (RRID:BDSC_30840), C232 (RRID:BDSC_30828), and R44D11-LexA (RRID:BDSC_41264), UAS-dTrpA1 (RRID:BDSC_26263), UAS-mCD8::GFP (RRID:BDSC_5136), UAS-mCD8::RFP, LexAop2-mCD8::GFP (RRID:BDSC_32229), and LexAop-Gal80 (RRID:BDSC_32213) were ordered from the Bloomington Drosophila Stock Center. GAL4 lines: VT012446, VT026841, VT042577, VT042759, VT045108, VT057257, VT038828, VT040539, and VT059775 were ordered from Vienna Drosophila Resource Center originally, but unfortunately not available anymore. 5HT7-GAL4 was provided by Charles Nicols' laboratory. Feb170-GAL4 was generated by Günter Korge's laboratory (Siegmond and Korge, 2001). The WT line w^{CS} was crossed with GAL4 and UAS parental lines as genetic controls. Experimental groups were from the F1 generation of crosses of GAL4 lines to UAS-dTrpA1.

Experimental design for sleep assays and calculation of sleep changes. F1 generation of flies were all maintained on standard food at 23°C. Two- to 5-day-old mated F1 female flies were individually placed into a 65 mm × 5 mm glass tube containing food (2% agar and 5% sucrose). After loading to the DAM2 system (Drosophila Activity Monitor) (Trikinetics; <https://www.trikinetics.com/>) at 21°C in 12 h:12 h light/dark cycles, flies were entrained for 2–3 d. Then 1 d baseline sleep, 1 d neural activation sleep, as well as 1 d recovery sleep were recorded at 21°C, 30°C, and 21°C, respectively. Total sleep, the number of sleep episodes, and maximum episode length were analyzed for light and dark periods (LP and DP) separately, using MATLAB (RRID:SCR_001622) program (SCAMP2019v2) scripts.

To overview the effects on activation of GAL4⁺ neurons, all genotypes were arranged in a descending order according to the changes of total sleep during the LP. Sleep changes were calculated by subtracting baseline day sleep of each genotype from its activation day. Since using TRPA1 to activate neurons requires an elevation of ambient temperature (above 25°C), and temperature has been shown to effect sleep (Parisky et al., 2016; Jin et al., 2021; Alpert et al., 2022), it is critical to compare with control groups that have undergone the same temperature shift. With genetic control groups and a subtraction to the baseline day, the temperature effect can be removed and sleep changes because of activation of the neurons can be quantified. For genotypes with significant changes in sleep and/or sleep structure, 3 days' sleep profiles of sleep time in 30 min were plotted. Sleep changes of the recovery day were also calculated. The significant difference was marked when the experimental group is different compared with both genetic controls.

Immunohistochemistry. Brains of adult flies were dissected in 10 mM ice-cold PBS and fixed for 20 min in PBS with 4% PFA at room temperature. Brains were then washed 3 times for 5 min each in PBT (PBS with 0.5% Triton X-100). For GFP and RFP immunostaining, brains were incubated with primary antibodies (1:200, chicken anti-GFP, Abcam, catalog #ab13970, RRID:AB_300798; 1:200, mouse anti-GFP, Roche, catalog #11814460001, RRID:AB_390913; 1:1000, rabbit anti-GFP, Invitrogen, catalog #A-11122, RRID:AB_221569; 1:200, rabbit anti-DsRed, Takara, catalog #632496, RRID:AB_10013483) in 10% NGS in PBT at 4°C for two nights. After 3 times washes for 5 min each with PBT at room temperature, brains were incubated with secondary antibody at 4°C overnight. Second antibodies (488 goat anti-mouse, Invitrogen, catalog #A-11001, RRID:AB_2534069; 488 goat anti-chicken, Invitrogen, catalog #A-11039, RRID:AB_142924; 488 goat anti-rabbit, In-

Table 1. Continued

Driver	LP (Fig. 1F)										DP (Fig. 1K)					
	Nonparametric/parametric test					Post hoc comparisons					Nonparametric/parametric test			Post hoc comparisons		
	Test	Dfn, Dfd	F	p		n1	n2	Mean difference	p		Test	F	p	Mean difference	p	
R73A06	K-W	3120	77.72	<0.0001	1 vs 2	25	32	−4.016	>0.9999	NS	K-W	15.11	0.0005	10.21	0.5429	NS
					1 vs 3	25	63	53.74	<0.0001	****				29.44	0.0007	***
Feb170	K-W	3,81	21.73	<0.0001	1 vs 2	29	25	26.48	<0.0001	****	K-W	52.79	<0.0001	33.97	<0.0001	****
					1 vs 3	29	27	24.31	0.0002	***				43.34	<0.0001	****
R70B05	K-W	3,89	29.88	<0.0001	1 vs 2	27	30	30.76	<0.0001	****	K-W	53.64	<0.0001	45.1	<0.0001	****
					1 vs 3	27	32	34	<0.0001	****				42.08	<0.0001	****

^aChange in sleep parameters for total sleep, number of episodes, maximum episode length, P(doze), and P(wake) on the activation day (30°C) were analyzed for day (LP) and night (DP) separately. Datasets that had a normal distribution, one-way ANOVA followed by Bonferroni test was applied. For datasets that did not pass the normality test, Kruskal–Wallis (K-W) followed by Dunn's test was applied. Post hoc tests were applied between the experimental group (F1 generation of the cross of GAL4 lines to UAS-dTrpA1)(1) and the genetic control groups (F1 generation of the crosses of either GAL4 lines to w^{CS} or UAS-dTrpA1 to w^{CS})(2 or 3). **p* < 0.05. ***p* < 0.01. ****p* < 0.001. *****p* < 0.0001.

vitrogen, catalog #A-11008, RRID:AB_143165; 568 goat anti-rabbit, Fisher Scientific, catalog #A-11011, RRID:AB_143157) were all used in a ratio of 1:200. Samples were then washed 3 times for 5 min each in PBT at room temperature, and mounted on microscope slide in Vectashield mounting medium (Vector Laboratories catalog #H-1000, RRID:AB_2336789). Finally, samples were imaged with Leica TCS SP5/LSM900 confocal microscope (RRID:SCR_002140) and analyzed using the open source of FIJI (ImageJ) software (RRID:SCR_002285).

Probability analysis. The probability of transitioning from a sleep to an awake state (P(wake)), and from a wake state to a sleep state (P(doze)) was used power law distributions analysis as previously described (Wiggin et al., 2020). P(wake) and P(doze) were calculated identically, with calculation of 1 min bin of inactivity and activity reversed. The MATLAB scripts for analysis of P(wake)/P(doze) can be accessed in GitHub at https://github.com/Griffith-Lab/Fly_Sleep_Probability.

Mixed Gaussian model clustering. To figure out different effects of EB drivers on both sleep pressure and depth, we divided all significant subtypes of EB ring neurons into groups with similar distributions of δ P(Wake) and δ P(Doze), using mixed Gaussian model clustering. The clustering analysis was conducted using the scripts of fitgmdist and cluster in MATLAB. Given the small sample size of neuron subtypes (14 and 13 for daytime and nighttime, respectively), the number of cluster *k* was set to 3, 4, or 5 for both daytime and nighttime. We calculated the silhouette coefficients for each *k* value using the script of silhouette in MATLAB and chose the final *k* value whose silhouette coefficient was the closest to one (Lecompte et al., 1986). The size of ellipse for each cluster was decided by the corresponding σ values of its Gaussian mixture distribution.

GLM. To evaluate the effect of a specific anatomic subtype of ring neurons on sleep, the GLM (Generalized linear models) was used to estimate the weights and the corresponding statistical significance of all subtypes for each sleep parameter. The GLM analysis was conducted using the script of glmfit in MATLAB (The MathWorks) to predict each sleep parameter under the combination of all subtypes of neurons. The input variable was defined as 1 or 0 for each subtype of ring neurons (R1, R2, R3d, R3m, R3a, R3p, R3w, R4m, R4d, R5, and R6) when labeled or not labeled by each driver, respectively. And the corresponding output variable was the mean change rate of each sleep parameter of the same driver on the activation to its baseline level (output variable value = (activation – baseline)/baseline). We chose the default parameters for the script of glmfit. According to the weight calculation for each subtype (see Table 6), a positive value represents positive relationship, and a negative value represents negative relationship between the subtype and the sleep parameter, respectively, when the corresponding *p* value < 0.05.

Statistical analysis. Power analysis was conducted using the script of sampsizepwr in MATLAB (The MathWorks) to calculate the power for the sample size in this study. The power analysis was based on the sleep parameters in drivers with significant differences from both control groups presented in the main figures. We selected the mean and SD of control groups under the null hypothesis, and the mean value of experimental groups under the alternative hypothesis during the calculation

of power values. Based on current sample size, >80% of the powers of significances of sleep parameters were >0.9 (see Tables 2 and 7).

Data were performed using GraphPad Prism 8 (RRID:SCR_002798). Group means were compared using one-way ANOVA followed by Bonferroni's multiple comparison test when data were normally distributed, or Kruskal–Wallis test followed by Dunn's multiple comparison test was used when data failed passing normality test (see Tables 1, 3, 4, 8, and 9). All experiments were performed at least 2 replicates, and data presented in the figures were chosen from one representative replicate. To uniform the data presentation, all figures were prepared as mean \pm SEM. To visualize all groups in the same figure clearer, error bars were not shown.

Results

Thermoactivation of ring neurons changes sleep amount

To investigate the roles of ring neuron types, we collected 34 GAL4 drivers that label different populations of ring neurons and used them to drive the thermogenetic tool dTrpA1, allowing the use of elevated temperature to drive neuronal firing (Hamada et al., 2008). Animals were placed in DAM2 system tubes and entrained at 21°C in a 12 h:12 h light/dark cycle. Sleep was then recorded for 3 d: 1 d of baseline sleep at 21°C, 1 d of neural activation sleep at 30°C, then 1 d of recovery sleep at 21°C (Fig. 1A). Changes in sleep parameters for each genotype on the activation and recovery days were calculated by subtracting the baseline day value (Fig. 1A). Changes were only considered significant when the experimental group was different from both genetic controls. Changes in total daytime sleep of the 34 drivers on the activation day are arranged in descending order (Fig. 1B), and changes of total nighttime sleep (Fig. 1G) as well as changes in the number of episodes (Fig. 1C,H), maximum episode duration (Fig. 1D,I), P(doze) (Fig. 1E,J), and P(wake) (Fig. 1F,K) are displayed in the same order as the daytime sleep data to allow assessment of all parameter changes for each genotype. The color-coding of the histogram bars corresponds to the Gaussian clusters shown in Figure 5 and is also used to identify lines in Figures 2, 3, 6, and 7 as part of particular clusters.

Activation of GAL4⁺ neurons produced many different patterns of change in the amount of sleep. During the daytime, a significant increase in total sleep was found when R47F07-GAL4⁺, R28E01-GAL4⁺, C232-GAL4⁺, and R56C09-GAL4⁺ neurons were activated (Fig. 1B; Table 1). Since change in total sleep is often associated with change in sleep structure (C. Liu et al., 2019; Wiggin et al., 2020), we also evaluated the number of sleep episodes, episode length, and the behavioral transition probabilities, P(doze) and P(wake) (Wiggin et al., 2020) to further understand the changes in sleep drive and arousal threshold. The increased

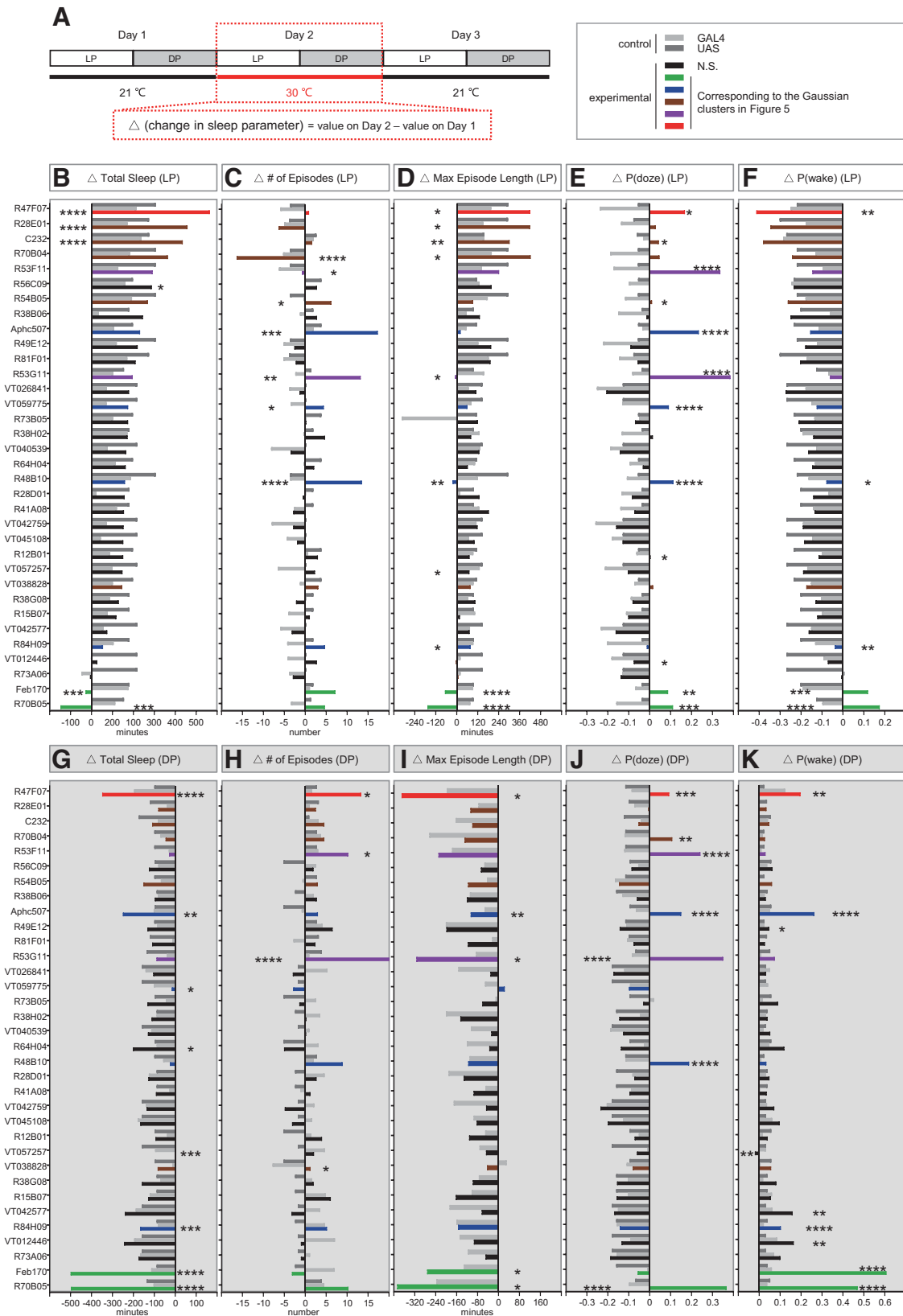


Figure 1. Sleep changes with activation of subtypes of ring neurons. **A**, Design of the experiments and calculation of sleep parameters on the activation day (red dashed box). **B, G**, Changes in sleep amount during day (LP) and night (DP). **C, H**, Changes in number of sleep episodes during daytime and night. **D, I**, Changes in maximum sleep episodes during daytime and night. **E, J**, Changes in P(doze) during daytime and night. **F, K**, Changes in P(wake) during daytime and night. Colored and black bars represent the experimental groups. Color codes are consistent through all of the figures and are based on the daytime cluster analysis in Figure 5. Gray and dark gray bars represent GAL4 control and UAS control, respectively. One-way ANOVA analysis and Dunn’s multiple comparisons test were used. Significance, only when the experimental group is significantly different from both GAL4 and UAS controls: * $p < 0.05$. ** $p < 0.01$. *** $p < 0.001$. **** $p < 0.0001$. Data are mean.

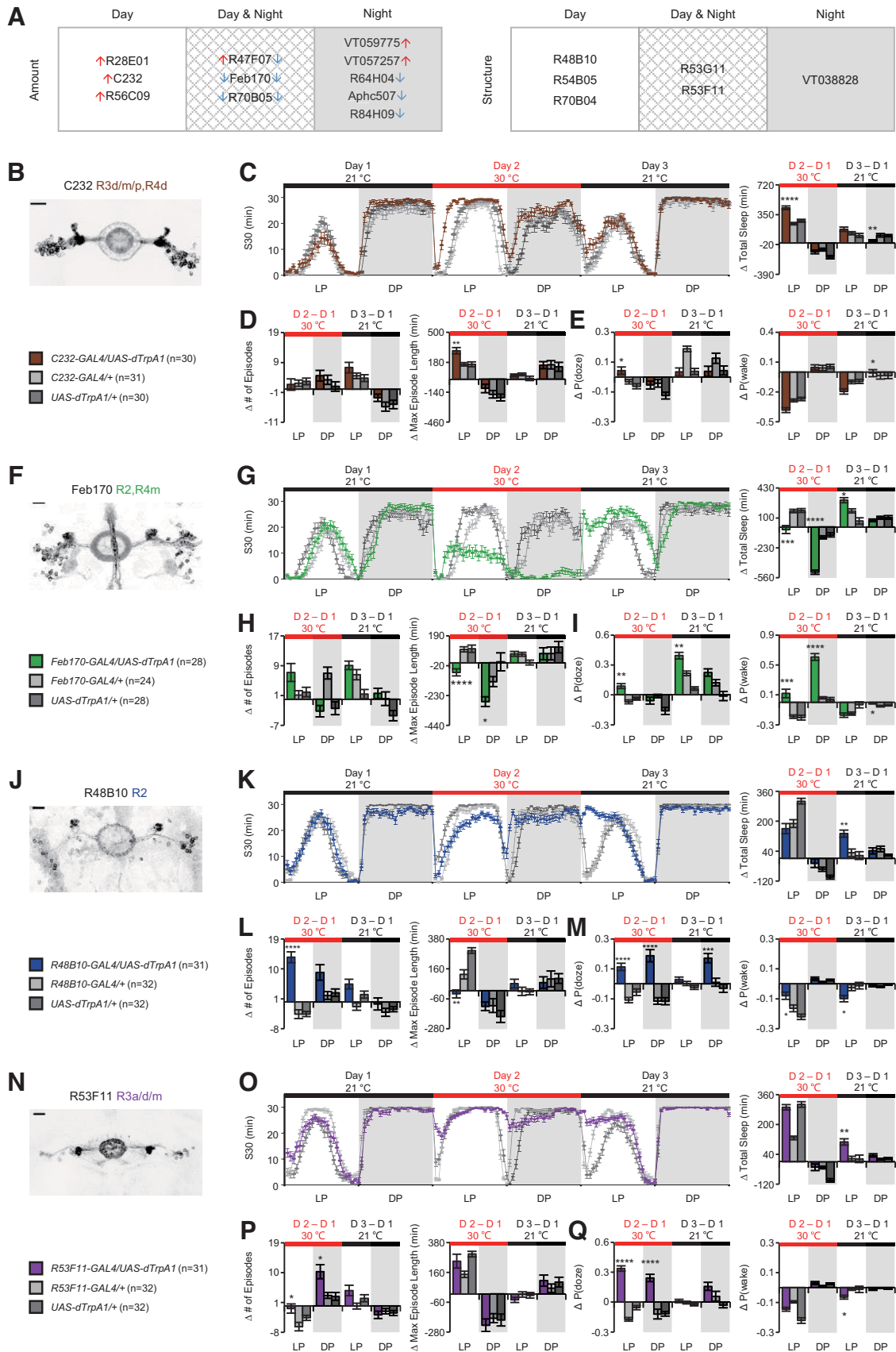


Figure 2. Complex effects on sleep homeostasis with thermoactivation of ring neurons. **A**, Summary of the drivers exhibited significant changes in total amount of sleep and sleep structure, respectively. Arrows on the left and right represent changes during the day and night, respectively. Up arrows represent increased total amount of sleep. Down arrows represent decreased total amount of sleep. Clusters represent the phenotypes observed day only, night only, or both day and night. Expression patterns of *c232-GAL4* (**B**), *Feb170-GAL4* (**F**), *R48B10-GAL4* (**J**), and

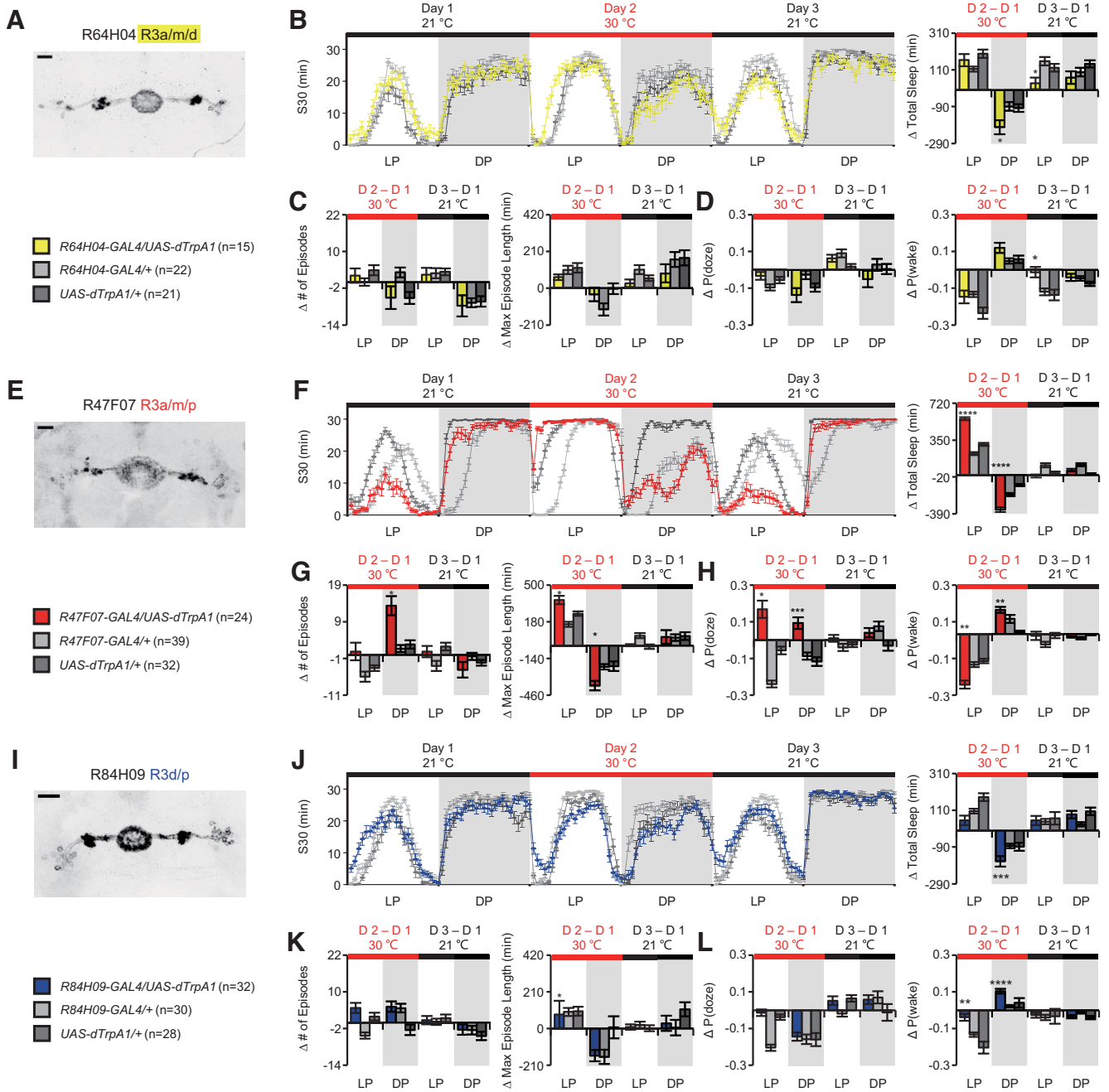


Figure 3. Complex effects on sleep homeostasis with thermoactivation of ring neurons. **A–D**, Decreased nighttime sleep often fails to induce rebound sleep on cessation of thermoactivation of ring neurons. **A**, Expression pattern of R64H04-GAL4 which labels R3a, R3m, and R3d neurons. **B**, Sleep profile and quantification of total sleep before, during, and after activation. Activation of R64H04-GAL4⁺ neurons reduced total sleep at night, and a persisting reduced sleep on cessation of activation. **C**, No significant change was observed in the number of episodes and maximum episode length. **D**, No change of P(doze) was observed, and significantly higher change in P(wake) than controls was found on cessation of activation. **E–L**, Drivers involved in the regulation of sleep amount and/or structure do not exhibit homeostatic rebound on cessation of thermoactivation. Expression pattern, sleep profile, quantification of sleep amount, sleep structure, and sleep drive/arousal threshold of each driver were presented. **E–H**, R47F07-GAL4. **I–L**, R84H09-GAL4. **p* < 0.05. ***p* < 0.01. ****p* < 0.001. *****p* < 0.0001. Data are mean ± SEM. Scale bar: 20 μm.

sleep observed in the above three drivers was accompanied by a significant increase in maximum episode length but no change in the number of episodes compared with their genetic controls (Fig. 1C,D). These flies had increased P(doze) and decreased

P(wake), suggesting that these neurons possibly contribute to increased sleep pressure and sleep depth (Fig. 1E,F).

We also found cell groups which, when activated, induced a significant reduction in total sleep: Feb170-GAL4⁺ and R70B05-GAL4⁺ neurons (Fig. 1B; Table 1). Sleep reduction was associated with significant decreases in maximum episode length with no change in the number of episodes compared with their genetic controls (Fig. 1C,D; Table 1). The reduced sleep amount and episode length were possibly because of the increased P(doze) and P(wake) (Fig. 1E,F; Table 1), suggesting neurons

←

R53F11-GAL4 (**M**). Sleep profiles with quantification of changes of sleep parameters of each driver: total sleep (**C,G,K,O**), the number of episodes and maximum episode length (**D,H,L,P**), and P(doze) and P(wake) (**E,I,J,M,Q**). Scale bar, 20 μm. **p* < 0.05. ***p* < 0.01. ****p* < 0.001. *****p* < 0.0001.

Table 2. Power analysis for the sample size of 4 drivers used in Figure 2^a

Total sleep	Experiment vs GAL4 Control				Experiment vs UAS Control			
	30°C		21°C		30°C		21°C	
	LP	DP	LP	DP	LP	DP	LP	DP
Drivers								
c232	1	0.167	0.377	0.639	1	0.563	0.533	0.907
Feb170	1	1	0.946	0.209	1	1	0.996	0.19
R48B10	0.151	0.53	0.934	0.077	1	0.998	0.975	0.999
R53F11	1	0.052	0.999	0.858	0.108	0.996	0.85	0.928

No. of episodes	Experiment vs GAL4 Control				Experiment vs UAS Control			
	30°C		21°C		30°C		21°C	
	LP	DP	LP	DP	LP	DP	LP	DP
Drivers								
c232	0.057	0.09	0.497	0.268	0.102	0.347	0.561	0.186
Feb170	0.929	0.99	0.234	0.083	0.819	0.06	0.989	0.86
R48B10	1	0.977	0.985	0.286	1	0.948	0.521	0.287
R53F11	0.816	1	0.948	0.149	0.705	0.992	0.323	0.078

Maximum episode length	Experiment vs GAL4 Control				Experiment vs UAS Control			
	30°C		21°C		30°C		21°C	
	LP	DP	LP	DP	LP	DP	LP	DP
Drivers								
c232	0.999	0.182	0.075	0.05	0.975	0.46	0.159	0.057
Feb170	1	0.795	0.053	0.05	0.993	0.859	0.673	0.121
R48B10	0.814	0.051	0.244	0.061	1	0.21	0.502	0.086
R53F11	0.815	0.188	0.275	0.219	0.413	0.091	0.19	0.054

^aFour GAL4 drivers were included in the analysis: c232, Feb170, R48B10, and R53F11. The experimental group was compared with either GAL4 control group or UAS-dTrpA1 control group for both activation day and recovery day. Total sleep, number of episodes, and maximum episode length for LP and DP were analyzed separately. Power analysis was conducted using the script of `sampsizepwr` in MATLAB.

labeled by these two drivers are involved in upregulation of sleep pressure and downregulation of sleep depth during the daytime.

Nighttime effects of thermogenetic neuron activation are more complex to interpret. Data have to be viewed in the context of the sleep-suppressing effects of elevated temperature on normal WT animal sleep (Parisky et al., 2016; Jin et al., 2021). This temperature effect can be visualized in the continuous sleep plots for most of the GAL4 and UAS control lines in Figures 2, 3, and 6. VT059775-GAL4⁺ and VT057257-GAL4⁺ neuron activation led to almost no change of total sleep compared with their own baseline, but this reflects a significant difference from genetic controls, which respond to heat with at large reduction in sleep. These lines also had only small reductions in P(wake) compared with controls, implying that these neurons may be involved in sleep promotion by changing sleep depth (Fig. 1G,K; Table 1).

We also found a number of GAL4 drivers, including R47F07, Aphc507, R64H04, R84H09, Feb170, and R70B05 which significantly reduced nighttime sleep amount compared with their controls, suggesting they contribute to promoting wakefulness (Fig. 1G; Table 1). These reductions in total sleep were accompanied by changes in sleep structure, featured as fragmentation where the number of episodes significantly increased and/or episode length reduced (Fig. 1H,I; Table 1). Many drivers exhibited increased P(doze) and P(wake) (Fig. 1J,K; Table 1), suggesting sleep pressure and sleep depth play important roles in nighttime sleep.

Thermoactivation of ring neurons can change sleep structure independent of sleep amount

We also found cases where sleep structure was changed without alterations in total sleep, supporting the idea that structure can be regulated independently (C. Liu et al., 2019). Activation of neurons from several GAL4 drivers, including R70B04, R53F11,

R54B05, R53G11, R48B10, and VT038828, resulted in significant change only in sleep structure. Except for R70B04, which induced consolidated daytime sleep with a decrease in the number of episodes and an increase in the episode length, all drivers mentioned above exhibited fragmented sleep either during the day or at night (Fig. 1C,D,H,I; Table 1). Fragmentation was accompanied by a robust increase in P(doze) for the majority drivers (Fig. 1E,J; Table 1). P(doze) is believed to correlate with sleep pressure (Wiggin et al., 2020), suggesting the fragmentation reflects an increase in the probability of switching from wake to sleep (i.e., high sleep drive rather than from an inability to maintain the sleep state).

The circadian period during which fragmentation occurred varied with GAL4 line. Daytime fragmentation was observed when R54B05-GAL4⁺ and R48B10-GAL4⁺ neurons were activated (Fig. 1C; Table 1), and nighttime fragmentation was seen when VT038828-GAL4⁺ neurons were activated (Fig. 1H; Table 1). Fragmentation of both day and night was found when R53G11-GAL4⁺ and R53F11-GAL4⁺ neurons were activated (Fig. 1C,D,H,I; Table 1).

The structural parameters that were altered were also variable. Three GAL4 drivers, R53F11, R54B05, and VT038828, only exhibited a significant increase in the number of episodes. R53G11 and R48B10 only showed reduced episode length. All of these changes contributed to increases in P(doze) with little or weak P(wake) effects, especially during the day (Fig. 1E,F,J,K; Table 1). Interestingly, R12B01-GAL4 did not exhibit detectable changes in the number of episodes or episode length, but had a significant increase in P(doze) compared with both controls (Fig. 1E; Table 1), suggesting a potential specific contribution of R28E01-GAL4⁺ neurons to control of sleep pressure. Together, changes in sleep structure are highly associated

Table 3. Statistical analysis of the recovery day for 4 drivers used in Figure 2^a

Driver	LP								DP					
	Nonparametric/parametric test				Post hoc comparisons				Nonparametric/parametric test			Post hoc comparisons		
	Test	DFn, DFd	F	p	n1	n2	Mean difference	p	Test	F	p	Mean difference	p	
D3-D1 21°C														
C232														
△ Total sleep	K-W	3,91	4.103	0.1285	1 vs 2	30 31	8.725	0.3943 NS	K-W	16.77	0.0002	−21.16	0.0035 **	
					1 vs 3	30 30	13.63	0.0912 NS				−26.32	0.0002 ***	
△ No. of episodes	K-W	3,91	4.451	0.108	1 vs 2	30 31	8.845	0.3803 NS	K-W	2.186	0.3352	9.984	0.2786 NS	
					1 vs 3	30 30	14.22	0.0735 NS				4.9	0.9435 NS	
△ Maximum episode length	K-W	3,91	1.39	0.4991	1 vs 2	30 31	−2.339	>0.9999 NS	K-W	0.326	0.8494	−1.673	>0.9999 NS	
					1 vs 3	30 30	5.45	0.8483 NS				2.183	>0.9999 NS	
△ P(doze)	K-W	3,92	28.85	<0.0001	1 vs 2	31 31	−30.23	<0.0001 ****	K-W	4.809	0.0903	−13.87	0.0817 NS	
					1 vs 3	31 30	2.694	>0.9999 NS				−2.237	>0.9999 NS	
△ P(wake)	K-W	3,92	5.069	0.0793	1 vs 2	31 31	−13.42	0.0957 NS	K-W	10.1	0.0064	17.19	0.0225 *	
					1 vs 3	31 30	−13.09	0.1112 NS				19.97	0.007 **	
Feb170														
△ Total sleep	K-W	3,80	27.64	<0.0001	1 vs 2	28 24	15.15	0.0382 *	K-W	3.219	0.2	−10.73	0.1939 NS	
					1 vs 3	28 28	32.63	<0.0001 ****				−8.661	0.3263 NS	
△ No. of episodes	ANOVA	2,77	9.999	0.0001	1 vs 2	28 24	2.488	0.1756 NS	ANOVA	4.401	0.0155	1.405	0.7464 NS	
					1 vs 3	28 28	7.679	<0.0001 ****				5.964	0.0108 *	
△ Maximum episode length	K-W	3,80	8.277	0.0159	1 vs 2	28 24	0.6994	>0.9999 NS	K-W	0.452	0.7979	−0.7917	>0.9999 NS	
					1 vs 3	28 28	15.98	0.0201 *				−3.964	>0.9999 NS	
△ P(doze)	K-W	3,81	44.43	<0.0001	1 vs 2	29 25	18.76	0.007 **	K-W	18.67	<0.0001	11.07	0.1695 NS	
					1 vs 3	29 27	41.91	<0.0001 ****				27.1	<0.0001 ****	
△ P(wake)	K-W	3,81	11.13	0.0038	1 vs 2	29 25	0.06207	>0.9999 NS	K-W	10.96	0.0042	19.4	0.005 **	
					1 vs 3	29 27	−18.47	0.0067 **				16.48	0.0176 *	
R48B10														
△ Total sleep	K-W	3,95	17.59	0.0002	1 vs 2	31 32	23.65	0.0013 **	K-W	0.76	0.684	−5.828	0.803 NS	
					1 vs 3	31 32	26.67	0.0002 ****				−1.546	>0.9999 NS	
△ No. of episodes	K-W	3,95	11.89	0.0026	1 vs 2	31 32	23.91	0.0011 **	K-W	4.2	0.1224	11.79	0.1781 NS	
					1 vs 3	31 32	12	0.167 NS				12.82	0.1289 NS	
△ Maximum episode length	K-W	3,95	2.567	0.2771	1 vs 2	31 32	8.717	0.4192 NS	K-W	1.002	0.606	−3.074	>0.9999 NS	
					1 vs 3	31 32	10.39	0.2696 NS				−6.933	0.6365 NS	
△ P(doze)	ANOVA	2,90	3.153	0.0475	1 vs 2	30 31	0.02628	0.4415 NS	ANOVA	13.58	<0.0001	0.1613	0.0003 ***	
					1 vs 3	30 32	0.05309	0.0277 *				0.2017	<0.0001 ****	
△ P(wake)	K-W	3,93	8.553	0.0139	1 vs 2	30 31	−16.77	0.0305 *	K-W	2.183	0.3357	10.15	0.2844 NS	
					1 vs 3	30 32	−18.15	0.0163 *				6.156	0.7389 NS	
R53F11														
△ Total sleep	K-W	3,95	15.56	0.0004	1 vs 2	31 32	23.22	0.0017 **	K-W	9.302	0.0096	20.46	0.0064 **	
					1 vs 3	31 32	24.33	0.0009 ****				5.681	0.8266 NS	
△ No. of episodes	K-W	3,95	7.201	0.0273	1 vs 2	31 32	18.6	0.0147 *	K-W	1.607	0.4479	−7.84	0.5069 NS	
					1 vs 3	31 32	10.08	0.2921 NS				−0.7308	>0.9999 NS	
△ Maximum episode length	K-W	3,95	1.743	0.4183	1 vs 2	31 32	−8.788	0.4117 NS	K-W	2.279	0.3201	8.549	0.4369 NS	
					1 vs 3	31 32	−6.726	0.6659 NS				−0.8881	>0.9999 NS	
△ P(doze)	ANOVA	2,95	1.461	0.2371	1 vs 2	30 34	0.01617	0.8543 NS	K-W	9.719	0.0078	9.725	0.3443 NS	
					1 vs 3	30 34	0.03458	0.183 NS				22.08	0.0039 **	
△ P(wake)	K-W	3,98	9.365	0.0093	1 vs 2	30 34	−19.12	0.0146 *	K-W	5.342	0.0692	−15.8	0.0531 NS	
					1 vs 3	30 34	−19.03	0.0151 *				−4.475	>0.9999 NS	

^aChange in sleep parameters, total sleep, number of episodes, maximum episode length, P(doze), and P(wake) on the recovery day (21°C) were analyzed for day (LP) and night (DP) separately. One-way ANOVA followed by Bonferroni test or Kruskal–Wallis (K-W) followed by Dunn's test was applied based on distribution of the datasets. **p* < 0.05. ***p* < 0.01. ****p* < 0.001. *****p* < 0.0001.

with P(doze), but when sleep structure changes are accompanied by changes in total sleep amount, P(wake) becomes an important component of the regulation.

Thermoactivation of ring neurons has complex effects on sleep homeostasis

We summarized drivers with significant changes of total amount of sleep or sleep structure during the day, at night, or both (Fig. 2A). We plotted sleep and changes in parameters over 3 d to provide a more nuanced picture of the lasting effects of activation of these neurons and present the lines ordered from largest to smallest rebound sleep on the recovery day (Figs. 2B–Q, 3; Tables 2–4). For some of the lines, the changes in total sleep

appeared to activate homeostatic changes that were evident during the recovery day. Activation of C232-GAL4⁺ neurons, which increases sleep on the activation day, leads to a negative rebound (decrease in sleep) on cessation of activation (Fig. 2C; Tables 2 and 3). Activation of Feb170-GAL4⁺ neurons decreased sleep both in the day and night, and this was followed by a homeostatic rebound increase in sleep (Fig. 2G; Tables 2 and 3). Activation of R48B10-GAL4⁺ or R53F11-GAL4⁺ neurons led to fragmentation during either the day or both in the day and night, and a robust homeostatic rebound increase occurred (Figs. 2J–Q; Tables 2 and 3). Interestingly, some drivers exhibited decreased sleep without a rebound change in sleep afterward (e.g., R64H04, R47F07, and R84H09; Fig. 3; Table 4), suggesting that, for these

Table 4. Statistical analysis of the recovery day for 3 drivers used in Figure 3^a

Driver	LP								DP					
	Nonparametric/parametric test				Post hoc comparisons				Nonparametric/parametric test			Post hoc comparisons		
	Test	Dfn, DFd	F	p	n1	n2	Mean difference	p	Test	F	p	Mean difference	p	
D3-D1 21°C														
R64H04														
△ Total sleep	ANOVA	2,55	5.451	0.0069	1 vs 2	15 22	−121.1	0.0035 **	ANOVA	2.027	0.1415	−29.82	0.6373 NS	
					1 vs 3	15 21	−85.58	0.0464 *				−75.3	0.0959 NS	
△ No. of episodes	ANOVA	2,55	0.0772	0.9258	1 vs 2	15 22	−0.5091	0.9676 NS	ANOVA	0.098	0.9072	−1.006	0.9253 NS	
					1 vs 3	15 21	−0.981	0.8884 NS				−1.4	0.8643 NS	
△ Maximum episode length	K-W	3,58	8.367	0.0152	1 vs 2	15 22	−16.35	0.0077 **	K-W	2.913	0.2331	−9.277	0.2017 NS	
					1 vs 3	15 21	−9.386	0.2003 NS				−7.681	0.3569 NS	
△ P(doze)	ANOVA	2,56	3.591	0.0341	1 vs 2	15 23	−0.02696	0.7393 NS	K-W	1.256	0.2927	−0.07932	0.2415 NS	
					1 vs 3	15 21	0.04529	0.2829 NS				−0.05507	0.5749 NS	
△ P(wake)	ANOVA	2,56	5.536	0.0064	1 vs 2	15 23	0.1066	0.016 *	K-W	3.68	0.1588	0.5768	>0.9999 NS	
					1 vs 3	15 21	0.124	0.0054 **				9.295	0.2188 NS	
R47F07														
△ Total sleep	ANOVA	2,92	7.799	0.0007	1 vs 2	24 39	−107.8	0.001 **	ANOVA	12.99	<0.0001	−54.83	0.0075 **	
					1 vs 3	24 32	−25.5	0.6125 NS				30.61	0.1952 NS	
△ No. of episodes	K-W	3,95	9.574	0.0083	1 vs 2	24 39	12.56	0.1576 NS	K-W	2.283	0.3194	−10.53	0.2796 NS	
					1 vs 3	24 32	−7.448	0.633 NS				−4.609	>0.9999 NS	
△ Maximum episode length	K-W	3,95	13.04	0.0015	1 vs 2	24 39	−20.25	0.0093 **	K-W	0.042	0.9793	−0.00641	>0.9999 NS	
					1 vs 3	24 32	0.8698	>0.9999 NS				−1.229	>0.9999 NS	
△ P(doze)	K-W	3,95	3.265	0.1954	1 vs 2	32 31	12.13	0.1615 NS	K-W	5.942	0.0513	−5.134	0.9198 NS	
					1 vs 3	32 32	8.75	0.4085 NS				11.38	0.1977 NS	
△ P(wake)	ANOVA	2,92	2.319	0.1041	1 vs 2	32 31	0.07036	0.1217 NS	K-W	9.721	0.0077	6.953	0.6339 NS	
					1 vs 3	32 32	−0.00178	0.9983 NS				−14.25	0.0774 NS	
R84H09														
△ Total sleep	K-W	3,90	0.3417	0.8429	1 vs 2	32 30	−2.221	>0.9999 NS	K-W	6.194	0.0452	10.71	0.2137 NS	
					1 vs 3	32 28	1.777	>0.9999 NS				−6.096	0.7344 NS	
△ No. of episodes	K-W	3,90	0.934	0.6269	1 vs 2	32 30	−0.725	>0.9999 NS	K-W	1.779	0.4108	1.976	>0.9999 NS	
					1 vs 3	32 28	−6.054	0.7396 NS				8.681	0.3972 NS	
△ Maximum episode length	K-W	3,90	1.147	0.5634	1 vs 2	32 30	−2.349	>0.9999 NS	K-W	1.838	0.399	1.258	>0.9999 NS	
					1 vs 3	32 28	4.877	0.9412 NS				−7.375	0.5506 NS	
△ P(doze)	K-W	3,88	8.562	0.0138	1 vs 2	31 30	12.25	0.1223 NS	K-W	2.214	0.3305	−1.055	>0.9999 NS	
					1 vs 3	31 27	−7.252	0.5617 NS				8.217	0.4435 NS	
△ P(wake)	K-W	3,88	0.9652	0.6172	1 vs 2	31 30	6.324	0.6676 NS	K-W	3.736	0.1545	−9.147	0.3242 NS	
					1 vs 3	31 27	2.068	>0.9999 NS				3.382	>0.9999 NS	

^aChange in sleep parameters, total sleep, number of episodes, maximum episode length, P(doze), and P(wake) on the recovery day (21°C) were analyzed for day (LP) and night (DP) separately. One-way ANOVA followed by Bonferroni test or Kruskal–Wallis (K-W) followed by Dunn's test was applied based on distribution of the datasets. **p* < 0.05. ***p* < 0.01.

lines, sleep loss was either not able to be compensated for or was not “counted” by the homeostat. These may represent cell types that are not integrated into the homeostat (Seidner et al., 2015).

Association of changes in arousal and sleep drive with GAL4⁺ groups of ring neurons

The majority of the GAL4 lines we screened contained more than one subtype of ring neuron (Fig. 4A), and exhibited expression outside the EB in other areas of the central brain (Table 5). To examine the linkage between ring neuron types and distinct aspects of sleep amount and/or sleep structure, we first separated drivers into two groups (Fig. 2A): (1) those that exhibited changes in sleep amount and (2) those that exhibited no change in sleep amount but had changes in sleep structure. Based on the time of day when the phenotype was observed (day only, night only, or both day and night), we classed those drivers into three clusters. For lines that changed total sleep, we noted their effects in Figure 2A as increasing or decreasing. The second type of information we layered into the analysis was the identification of the subtypes of ring neurons in each line according to anatomic features and recent nomenclature (Omoto et al., 2018; Hulse et al., 2021) (Fig. 4A). Based on this primary classification, many subtypes of ring neurons, including R1, R2,

R4m, R4d, R5, and many R3 subtypes (R3a, R3m, R3d, and R3p), may participate in the regulation of sleep amount (Fig. 4B). Because of the multiplicity of ring neurons in these EB drivers, it was hard to *a priori* link a single subtype of EB neuron with a specific function in the regulation of sleep amount/structure. Thus, we used statistical models to try to identify links between ring subtypes and phenotypes.

The first approach we used was aimed at determining the effects of the GAL4 lines (each of which has a different mixture of ring neuron subtypes) in regulating sleep. We used a mixed Gaussian model for changes in P(wake) or P(doze) on the activation day compared with the baseline day (Fig. 5A,B). We chose to use these transition probabilities since they capture some of the more complex aspects of sleep: P(wake) correlates with arousal state/sleep depth, while P(doze) is a measure of sleep drive (Wiggin et al., 2020). A single value of ΔP(wake) and ΔP(doze) for each line was calculated by subtracting the average of the genetic controls for that driver (experimental ΔP − (UAS ΔP + GAL4 ΔP)/2)). These values were then plotted in ΔP(wake)–ΔP(doze) space and clustered with the model to find groups with similar effects on sleep depth and pressure. We identified five clusters of GAL4 lines for day and night, respectively (Fig. 5A,B). These clusters define the color codes used in Figures 1, 2, 3, 5, 6 and Figure 7.

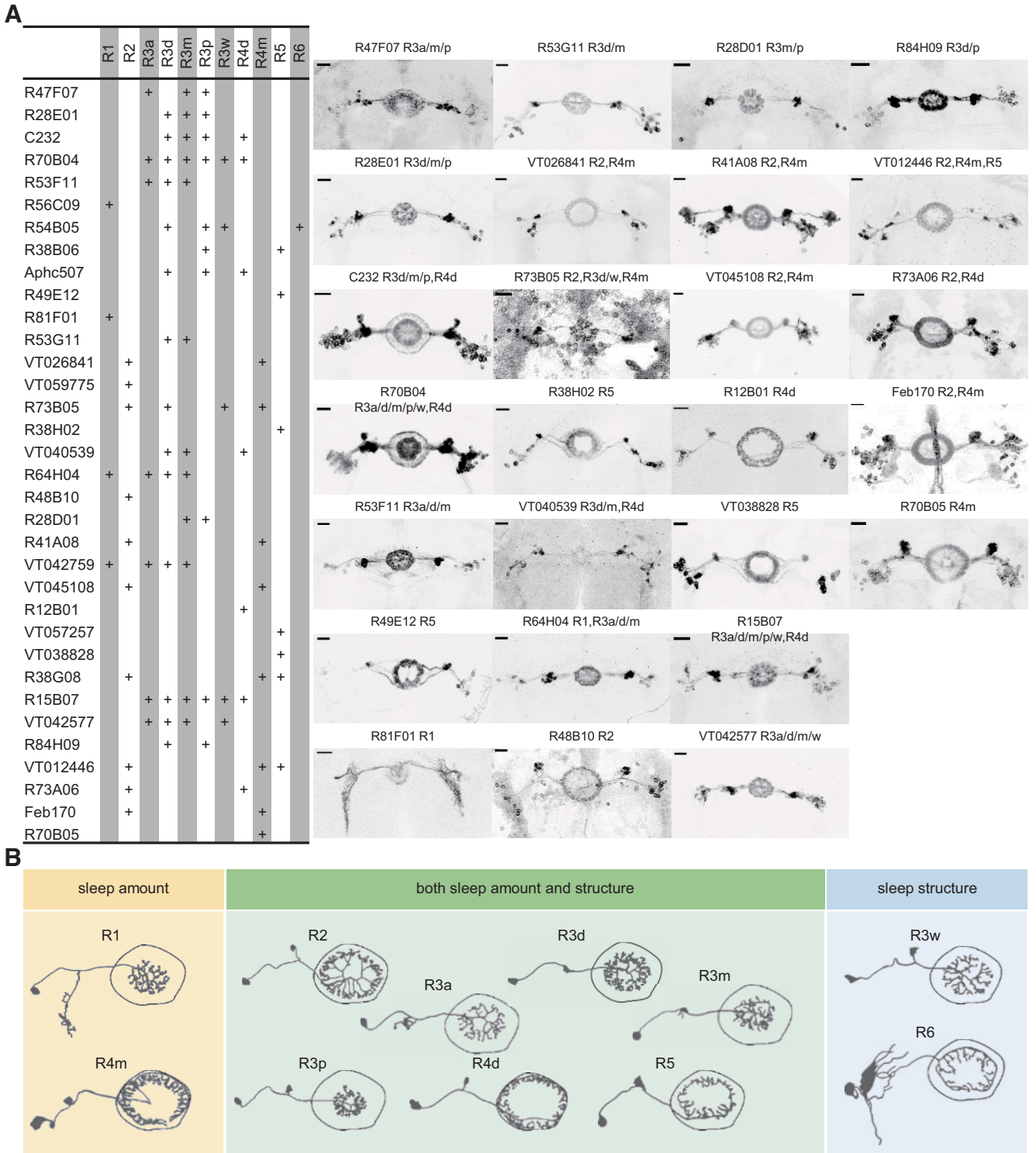


Figure 4. Expression patterns of EB drivers in the screen. **A**, Distinct subtypes of ring neurons were labeled by the 34 drivers. Expression patterns of all the publicly available drivers (26) are shown. **B**, Single subtype of ring neurons that are involved in the regulation of sleep amount (yellow), structure (blue), and both amount and structure (green). “+” in columns indicates where the driver has expression. Scale bar: 20 μ m.

Using our anatomic analysis of these lines, we found that the lines within each cluster shared a common ring neuron subtype. During the daytime (Fig. 5A), R4m (and perhaps R2 neurons) emerged as strong candidates for the regulation of sleep depth/arousal since they are present in lines that have high ΔP (wake) values. R3dm cells appeared to increase sleep drive (i.e., increase the probability of falling asleep); consistent with this, lines with

these cells had high P(doze). R2, R3d, and R3p neurons were present in several clusters and did not appear to have unique functionality with regard to sleep depth and drive, but a role in facilitation of the effects of R2 and R3m neurons, or in more specialized functions in sleep structure, cannot be ruled out. We also observed that many drivers play different roles during the day and night (Fig. 5B). For example, R70B05 exhibits relative strong

Table 5. Expression patterns of 34 drivers outside the EB in the central brain^a

	Sleep Amount	Sleep Structure	AL	AMMC	AOTU	ATL	AVLP	CL	FB	GA	GNG	ICL	LH	LO	LOP	MB	ME	NO	OL	PI	PRW	SAD	SCL	SEZ	SIP	SLP	SMP	WED	Ventrolateral protocerebrum	Adult pheromone projection PPN1 neuron	Large field neuron	Source	
R47F07	✓	✓									+			+	+		+															VF	
R28E01	✓																															FB	
C232	✓																														+	FB	
R70B04		✓																														FB	
R53F11		✓																														FB	
R56C09	✓																														+	FB	
R54B05	✓		+							+	+			+	+													+				VF	
R38B06																																FB	
Aphc507	✓	✓																													+	FB	
R49E12																																FB	
R81F01																																	VF
R53G11		✓	+		+			+		+				+	+											+	+		+	+	+	VF	
VT026841			+																													FB	
VT059775	✓	✓	+			+																										FB	
R73B05																																VF	
R38H02			+																													FB	
VT040539			+																													FB	
R64H04	✓																															FB	
R48B10		✓	+		+																											FB	
R28D01																																FB	
R41A08																																	FB
VT042759																																	FB
VT045108			+																														FB
R12B01																																	FB
VT057257	✓		+	+	+																												FB
VT038828		✓																															FB
R38G08																																	FB
R15B07																																	FB
VT042577																																	FB
R84H09	✓																																VF
VT012446																																	FB
R73A06																																	FB
Feb170	✓																																FB
R70B05	✓																																VF

^aDrivers are listed in the first column. ✓ (in the second or third column) indicates whether they had a phenotype for sleep amount and/or sleep structure. + (in subsequent columns) indicates where the driver has expression. The regions of the central brain were in abbreviation based on description of FlyBase and Virtual FlyBrain in alphabet order. AL, Antennal lobe; AMMC, antennal mechanosensory and motor center; AOTU, anterior optic tubercle; ATL, antler; AVLP, anterior ventrolateral protocerebrum; CL, clamp; GA, gall; GNG, gnathal ganglion; ICL, inferior clamp; LH, lateral horn; LO, lobula; LOP, lobula plate; ME, medulla; NO, nodulus; OL, optic lobe; PI, pars intercerebralis; PRW, prow; SAD, saddle; SCL, superior clamp; SEZ, subesophageal zone; SIP, superior intermediate protocerebrum; SLP, superior lateral protocerebrum; SMP, superior medial protocerebrum; WED, wedge. Source of images for expression analysis is listed in the last column. VF, virtual fly brain; FB, FlyBase. Non-EB expression was not predictive of either total sleep or sleep structure phenotypes.

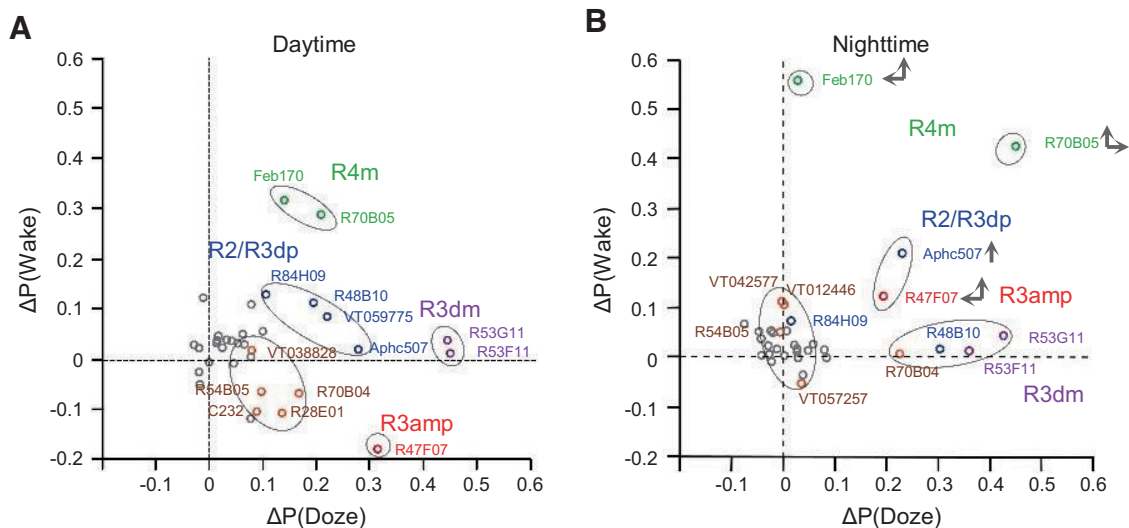


Figure 5. Association of changes in arousal and sleep drive with GAL4⁺ groups of ring neurons. Mixed Gaussian model cluster analysis for drivers have similar patterns during the daytime (**A**) and at night (**B**). Gray dots represent activation did not show significance in P(wake)/P(doze) analysis. Green dots represent increase in both P(wake) and P(doze). Blue dots represent mild increase in both P(wake) and P(doze). Brown dots represent weak increase in both P(wake) and P(doze). Purple dots represent increase only in P(doze). Red dots represent increase in P(doze) and decrease in P(wake). Vertical and horizontal arrows in nighttime panel represent shifts in location of P(doze) and P(wake) compared with the daytime.

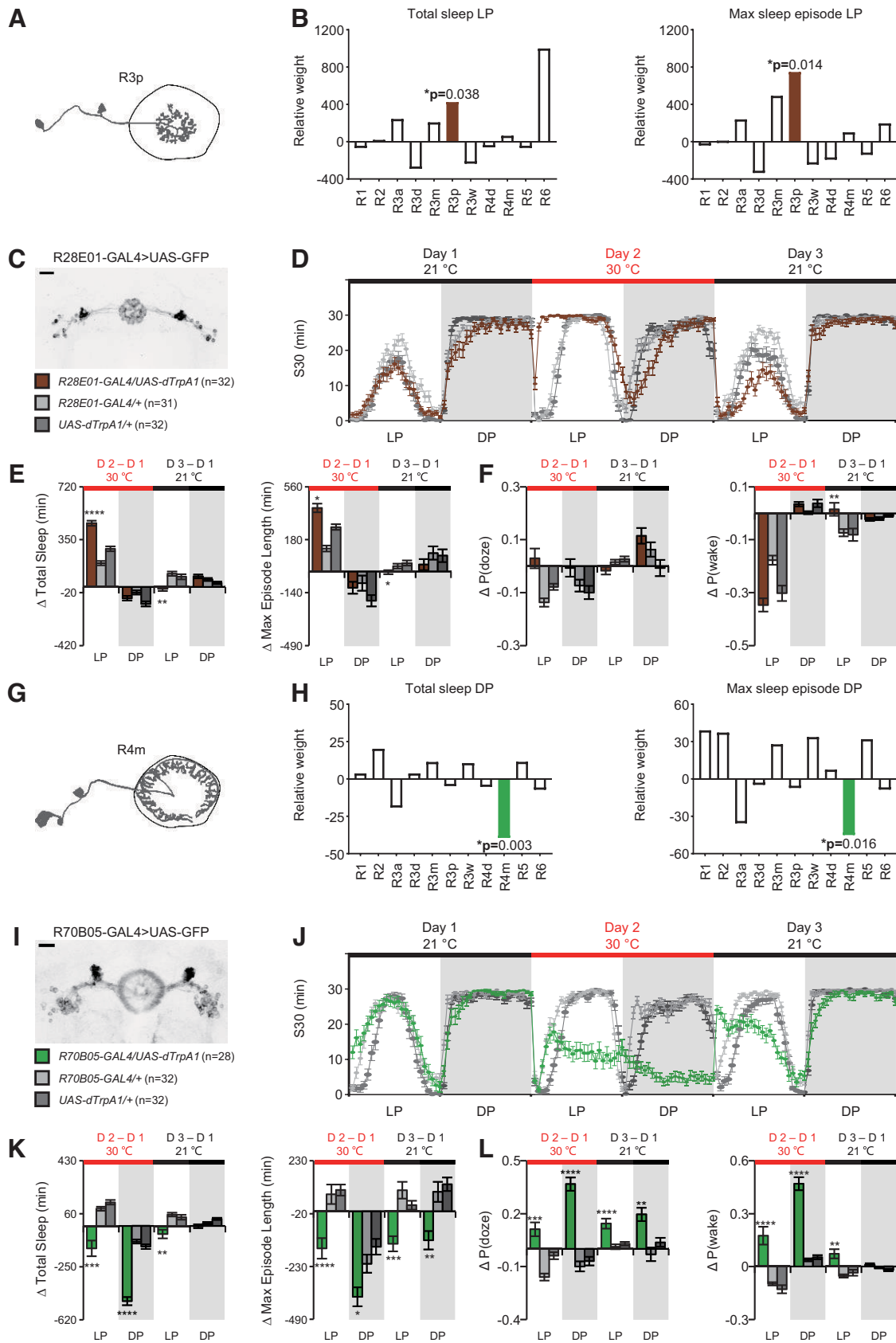


Figure 6. Two subtypes of ring neurons identified by GLM that significantly contribute in the regulation of total sleep and episode length. **A, G**, Schematic morphologic pattern of a single R3p neuron and R4m neuron, respectively. **B, H**, R3p neuron and R4m neuron are highly correlated to regulate daytime sleep and nighttime sleep, respectively. The weight of each subclass was analyzed with a GLM. **C, I**, Expression pattern of R28E01-GAL4 and R70B05-GAL4 as representative for R3p and R4m. **D, J**, Sleep profiles of total sleep before, during and after activation of R28E01-GAL4⁺ and R70B05-GAL4⁺ neurons with two controls. **E, K**, Changes in total amount of sleep and maximum episodes on the activation day and the recovery day. R70B05-GAL4⁺ neurons not only significantly reduced nighttime sleep but also exhibited strong impact on reducing daytime sleep. **F**, No detectable changes in P(doze) on and after activation of R28E01-GAL4⁺

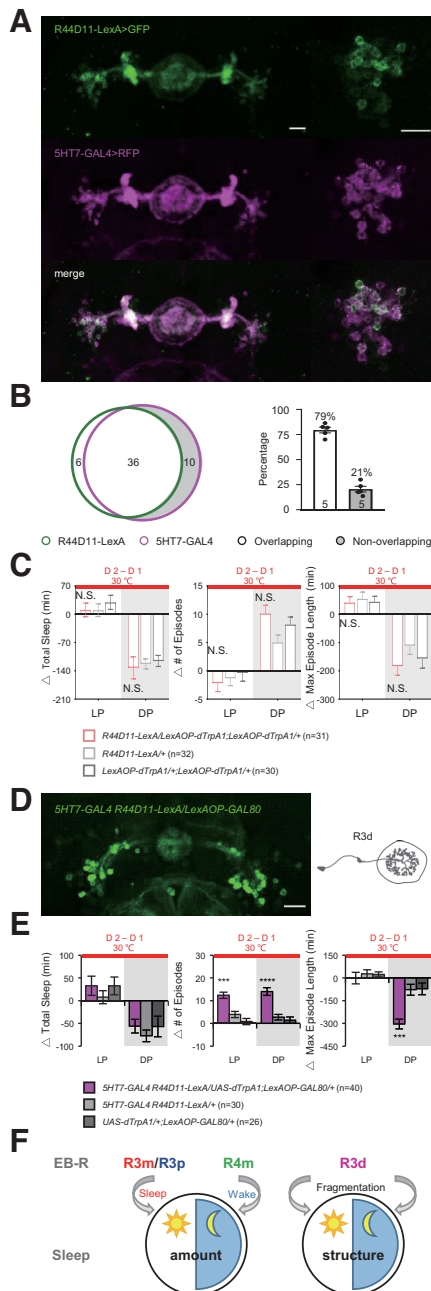


Figure 7. R3d neurons contribute to sleep fragmentation. **A**, Expression pattern of R44D11-LexA⁺ neurons and 5HT7-GAL4⁺ neurons labeled by GFP and RFP, respectively; 79% of the R44D11-LexA⁺ neurons (green) overlap with 5HT7-GAL4⁺ neurons (magenta). **B**, Venn diagram represents the overlapping and nonoverlapping cells between 5HT7-GAL4⁺ and R44D11-LexA⁺. Bar graph represents the quantified ratio of nonoverlapping neurons. **C**, Activation of R44D11-LexA⁺ neurons do not change sleep or sleep structure during both day and night. **D**, R3d populations are labeled by suppressing the overlapped neurons of R44D11-LexA⁺ and 5HT7-GAL4⁺ by using LexAOP-GAL80. Scale bar, 20 μ m. **E**, Activation of the nonoverlapping R3d neurons fragments sleep without significant effect on total amount during LP and DP. **F**, Schematic of sleep/structure regulation by multiple subtypes of ring neurons. *** $p < 0.001$. **** $p < 0.0001$. Data are mean \pm SEM.

←

neurons. Weak elevation of P(wake) on the recovery day was found. **L**, Strong increase in P(doze) was found when R70B05-GAL4⁺ neurons were activated, and this effect lasted with cessation of activation. Significant increase in P(wake) was also observed on and after activation. * $p < 0.05$. ** $p < 0.01$. *** $p < 0.001$. **** $p < 0.0001$. Data are mean \pm SEM. Scale bar: 20 μ m.

P(wake) but weak P(doze) effect during the day, but at night increases its influence on P(doze); R47F07 has little effect on P(wake) in the day but becomes much more wake-promoting at night.

Association of specific ring neuron subtypes with changes in sleep parameters

Since the variable analyzed using Gaussian clustering was the GAL4 line, which is most often a collection of different ring neuron subtypes, the effects we saw could also be the result of particular combinations of subtypes rather than the result of one dominant subtype alone. To try to isolate effects specific to subtypes, and to look at more specific sleep parameters, we used a second method to extract the contributions of each ring neuron subtype to functional outcomes. Using a GLM with ring neuron subtype as the variable allowed us to calculate the weights of the potential contribution of each subtype of ring neuron to all the sleep parameters for daytime and nighttime, respectively (Table 6). R3p exhibited a significantly positive effect on daytime sleep amount which was associated with its positive weight in episode length (Fig. 6A,B; Table 7). As an example, activation of R28E01-GAL4⁺ neurons, which include the R3p subtype, elevated daytime sleep and maximum episode length (Fig. 6C–E; Table 8). But the R3p subtype had little effect on P(doze) or P(wake) (Fig. 6F; Table 8). We also found that R4m had a significantly inhibiting effect on total sleep at night and a negative effect on episode length (Fig. 6G,H; Table 7), consistent with the results of Gaussian clustering. R70B05-GAL4⁺ neurons include the R4m subtype, and activation of neurons labeled by this driver caused a dramatic reduction of sleep in both day and night, which is likely because of the shortened episode length (Fig. 6I–K; Table 8). The effects of activation of these R70B05-GAL4⁺ neurons persisted into the recovery day, with flies exhibiting significantly elevated sleep pressure and lightened sleep depth (Fig. 6L; Table 8).

Ring neuron synergy is important for sculpting sleep

Interestingly, there were effects uncovered in the GLM analysis that were not seen with GAL4 drivers that labeled only that specific subtype. R1 and R2 neurons exhibit a significantly negative weight in the number of episodes at night, suggesting that these neurons may contribute to consolidation of sleep structure (Table 6). However, we failed to observe consolidation after activation of R1- or R2-specific GAL4 drivers; R56C09 and R81F01 had little significant effect on sleep structure (Fig. 1; Table 1), while activation of R48B10 produced a moderately strong increase in P(doze/wake) (Fig. 2M; Table 3). This suggests that the sleep consolidation effects of activating these neurons uncovered by the GLM requires coactivation of other subtypes.

Supporting the complexity of ring neuron subtype interactions, we observed that activation of the R47F07-GAL4 driver, which labels R3a, R3m, and R3p ring neurons, induced increased daytime sleep but reduced nighttime sleep (Figs. 3E,F, 5; Table 4). Increased daytime sleep was associated with an increase of episode length, explained by elevated sleep pressure and “deeper” sleep depth (Figs. 3G,H, 5; Table 4). Opposite to the daytime change, reduced nighttime sleep was accompanied by fragmentation, resulting in increased sleep pressure and/or light sleep depth (Figs. 3G,H, 5; Table 4). How these three subtypes of ring neurons coordinate to segregate, and effect a sign change on, day and night sleep still needs to be determined but may provide insight into coordination of the EB circuit.

Table 6. Statistical table of the weight of the effect of subclasses of ring neurons on the sleep using a GLM^a

Subtype	Total sleep				No. of episodes				Maximum episode length			
	LP		DP		LP		DP		LP		DP	
	Weight	<i>p</i>	Weight	<i>p</i>	Weight	<i>p</i>	Weight	<i>p</i>	Weight	<i>p</i>	Weight	<i>p</i>
R1	−66.963	0.806	3.71	0.789	−78.081	0.218	−289.982	0.025*	−40.711	0.918	39.093	0.058
R2	−4.43	0.986	20.206	0.117	−53.171	0.351	−287.956	0.015*	10.987	0.976	37.288	0.047*
R3a	243.881	0.394	−19.084	0.192	0.156	0.998	100.72	0.43	239.529	0.562	−35.538	0.095
R3d	−290.368	0.202	3.727	0.742	72.222	0.166	−99.637	0.323	−335.803	0.306	−4.78	0.769
R3m	207.085	0.45	11.389	0.413	−110.33	0.086	97.25	0.428	490.865	0.222	27.874	0.168
R3p	424.718	0.038*	−4.8	0.628	12.879	0.772	−24.945	0.775	747.409	0.014*	−7.29	0.608
R3w	−235.362	0.422	10.664	0.472	−77.07	0.253	−118.224	0.367	−244.843	0.563	33.605	0.122
R4d	−60.809	0.768	−5.332	0.61	−23.994	0.611	−104.199	0.264	−192.1	0.522	7.413	0.621
R4m	63.512	0.793	−39.476	0.003*	−3.416	0.951	97.465	0.371	100.607	0.774	−45.005	0.016*
R5	−67.36	0.751	11.467	0.292	−49.769	0.31	−168.218	0.086	−140.881	0.648	31.922	0.048*
R6	999.282	0.069	−7.214	0.788	81.007	0.505	103.387	0.663	196.977	0.798	−8.583	0.823

^aThe generalized linear model (GLM) analysis was conducted using the script of glmfit in MATLAB with the default parameters setting for total sleep, number of episodes, and maximum episode length. A positive value represents a positive relationship, and a negative value represents a negative relationship between the subtype of ring neurons and the sleep parameter, respectively. **p* < 0.05.

Table 7. Power analysis for the sample size of two drivers used in Figure 6^a

Total sleep	Experiment vs GAL4 Control				Experiment vs UAS Control			
	30°C		21°C		30°C		21°C	
	LP	DP	LP	DP	LP	DP	LP	DP
Drivers								
R28E01	1	0.511	0.999	0.28	1	0.313	0.9	0.951
R70B05	1	1	1	0.667	1	1	0.994	0.985

No. of episodes	Experiment vs GAL4 Control				Experiment vs UAS Control			
	30°C		21°C		30°C		21°C	
	LP	DP	LP	DP	LP	DP	LP	DP
Drivers								
R28E01	0.116	0.101	0.198	0.233	0.425	0.074	0.214	0.121
R70B05	0.992	0.888	1	0.994	0.47	0.878	1	0.997

Maximum episode length	Experiment vs GAL4 Control				Experiment vs UAS Control			
	30°C		21°C		30°C		21°C	
	LP	DP	LP	DP	LP	DP	LP	DP
Drivers								
R28E01	1	0.07	0.425	0.222	0.995	0.354	0.659	0.161
R70B05	0.947	0.652	0.981	0.873	1	0.983	1	1

^aTwo GAL4 drivers were included in the analysis: R28E01 and R70B05. The experimental group was compared with either GAL4 control group or UAS-dTrpA1 control group for both activation day and recovery day. Total sleep, number of episodes, and maximum episode length for LP and DP were analyzed separately. Power analysis was conducted using the script of sampsizepwr in MATLAB.

Regulation of sleep fragmentation by a specific ring neuron subset

One of the interesting findings of this screen was that there appeared to be circuits that regulate sleep structure independent of sleep amount. These data were consistent with our previous studies, which identified 5HT in EB as a modulator of sleep structure; activation of 5HT7-GAL4⁺ neurons fragmented sleep without changing the amount of sleep (C. Liu et al., 2019). 5HT7-GAL4⁺ neurons include R3d, R3p, and R4d subtypes (Hulse et al., 2021). To examine whether sleep structure regulation could be attributed to a specific subtype, we identified a driver R44D11-LexA that had an expression pattern similar to 5HT7-GAL4 (Fig. 7A). LexA⁺ neurons overlapped nearly 79% with 5HT7-GAL4⁺ neurons (Fig. 7B), but activation of R44D11-LexA⁺ neurons does not induce sleep/structure changes on activation (Fig. 7C; Table 9). To test the hypothesis that sleep fragmentation might be induced by the nonoverlapping population of 5HT7-GAL4⁺ neurons, we introduced LexAop-GAL80 to

suppress the overlapping neurons between R44D11-LexA⁺ and 5HT7-GAL4⁺ neurons (Fig. 7D). We found that activation of the nonoverlapping 5HT7-GAL4⁺ neurons increased the number of episodes and reduced episode length (Fig. 7E; Table 9), suggesting that the nonoverlapping neurons play a critical role in sleep fragmentation. Interestingly, the nonoverlapping neurons morphologically are R3d subtypes (Fig. 7D). This subtype of ring neuron was present in 4 of 6 of the lines we identified in this screen as affecting structure only (R70B04, R53F11, R54B05, R53G11), and there were also R3d neurons in some lines that fragmented sleep in addition to changing its amount (Aphc507, R84H09). The fact that not all lines that contain this ring neuron subtype fragment sleep may be because of interactions with other ring neuron types or heterogeneity within the R3d population.

Discussion

Sleep is crucial for survival and overall health across animal kingdoms. Fly sleep exhibits the majority of the highly conserved

Table 8. Statistical analysis of the recovery day for two drivers used in Figure 6^a

Driver	LP								DP						
	Nonparametric/parametric test				Post hoc comparisons				Nonparametric/parametric test			Post hoc comparisons			
	Test	DFn, DFd	F	p	n1	n2	Mean difference	p	Test	F	p	Mean difference	p		
D3-D1 21°C															
R28E01															
△ Total sleep	K-W	3,95	22	<0.0001	1 vs 2	32 31	−31.06	<0.0001	****	K-W	4.966	0.0835	5.503	0.8565	NS
					1 vs 3	32 32	−23.77	0.0011	**				15.17	0.0554	NS
△ Maximum episode length	K-W	3,95	7.5	0.0235	1 vs 2	32 31	−15.71	0.0474	*	K-W	1.406	0.4951	−7.219	0.5974	NS
					1 vs 3	32 32	−16.97	0.0276	*				−6.969	0.6239	NS
△ P(doze)	K-W	3,96	4.376	0.1121	1 vs 2	32 32	−7.656	0.5432	NS	K-W	8	0.0183	9.281	0.3653	NS
					1 vs 3	32 32	−14.56	0.073	NS				19.69	0.0094	**
△ P(wake)	K-W	3,96	12.76	0.0017	1 vs 2	32 32	22.16	0.0029	**	K-W	2.335	0.3111	−2.031	>0.9999	NS
					1 vs 3	32 32	20.88	0.0054	**				−10.06	0.297	NS
R70B05															
△ Total sleep	K-W	3,92	16.31	0.0003	1 vs 2	28 32	−26.52	0.0002	***	K-W	13.3	0.0013	−7.692	0.5311	NS
					1 vs 3	28 32	−21.48	0.0038	**				−24.4	0.0008	***
△ Maximum episode length	K-W	3,92	27.48	<0.0001	1 vs 2	28 32	−35.09	<0.0001	****	K-W	20.64	<0.0001	−23.01	0.0017	**
					1 vs 3	28 32	−26.31	0.0003	***				−30.33	<0.0001	****
△ P(doze)	ANOVA	2,86	14.35	<0.0001	1 vs 2	27 30	0.1319	<0.0001	****	ANOVA	10.82	<0.0001	0.2261	<0.0001	****
					1 vs 3	27 32	0.1144	<0.0001	****				0.1582	0.0035	**
△ P(wake)	K-W	3,89	18.94	<0.0001	1 vs 2	27 30	28.97	<0.0001	****	K-W	14.74	0.0006	15.24	0.0523	NS
					1 vs 3	27 32	21.15	0.0035	**				25.88	0.0003	***

^aChange in sleep parameters, total sleep, number of episodes, maximum episode length, P(doze), and P(wake) on the recovery day (21°C) were analyzed for day (LP) and night (DP) separately. One-way ANOVA followed by Bonferroni test or Kruskal–Wallis (K-W) followed by Dunn's test was applied based on distribution of the datasets. **p* < 0.05. ***p* < 0.01. ****p* < 0.001. *****p* < 0.0001.

Table 9. Statistical analysis of the activation day for two drivers used in Figure 7^a

Driver	LP								DP						
	Nonparametric/parametric test				Post hoc comparisons				Nonparametric/parametric test			Post hoc comparisons			
	Test	DFn, DFd	F	p	n1	n2	Mean difference	p	Test	F	p	Mean difference	p		
D3-D1 21°C															
Figure 7C															
△ Total sleep	K-W	3,93	2.44	0.2952	1 vs 2	31 32	0.2535	>0.9999	NS	K-W	4.394	0.1111	−10.63	0.2363	NS
					1 vs 3	31 30	−9.22	0.3644	NS				−13.76	0.0929	NS
△ No. of episodes	K-W	3,93	0.7446	0.6892	1 vs 2	31 32	−1.765	>0.9999	NS	K-W	7.075	0.0291	17.92	0.0167	*
					1 vs 3	31 30	−5.817	0.799	NS				7.035	0.6165	NS
△ Maximum episode length	K-W	3,93	0.1451	0.93	1 vs 2	31 32	−2.587	>0.9999	NS	ANOVA	1.287	0.281	−72.87	0.202	NS
					1 vs 3	31 30	−1.191	>0.9999	NS				−26.9	0.7888	NS
Figure 7E															
△ Total sleep	ANOVA	2,93	0.5201	0.5962	1 vs 2	40 30	25.21	0.5593	NS	K-W	1.289	0.525	7.621	0.5146	NS
					1 vs 3	40 26	0.2596	>0.9999	NS				2.791	>0.9999	NS
△ No. of episodes	K-W	3,96	27.92	<0.0001	1 vs 2	40 30	24.85	0.0004	***	ANOVA	21.09	<0.0001	11.26	<0.0001	****
					1 vs 3	40 26	34.78	<0.0001	****				12.6	<0.0001	****
△ Maximum episode length	K-W	3,96	1.574	0.4551	1 vs 2	40 30	−5.592	0.8118	NS	K-W	20.92	<0.0001	−25.46	0.0003	***
					1 vs 3	40 26	−8.41	0.4615	NS				−27.34	0.0002	***

^aChange in sleep parameters, total sleep, number of episodes, and maximum episode length on the activation day (30°C) were analyzed for LP and DP separately. One-way ANOVA followed by Bonferroni test or Kruskal–Wallis (K-W) followed by Dunn's test was applied based on distribution of the datasets. **p* < 0.05. ****p* < 0.001. *****p* < 0.0001.

features of vertebrate sleep, and the tractability of *Drosophila* as an experimental model has produced a growing number of studies, which contribute to our knowledge of sleep mechanisms and circuits. In addition to the importance in learning and memory of the mushroom body (MB), multiple subtypes of intrinsic MB Kenyon cells (KCs) have been identified as influencing sleep (Joiner et al., 2006; Sitaraman et al., 2015; Artiushin and Sehgal, 2017; Bringmann, 2018). For example, $\alpha'\beta'$ and γ m KCs contribute to wake promotion, and γ d KCs contribute to sleep promotion (Sitaraman et al., 2015). A pair of GABAergic and serotonergic dorsal paired medial neurons, which are MB extrinsic projecting neurons and play a role in memory consolidation (Keene et al.,

2004, 2006; Zhang et al., 2013), were shown to be involved in promoting sleep (Haynes et al., 2015). Dopaminergic PPL1 and PPM3 neurons that project to different layers of fan-shaped body (FB) have been shown to have specific roles in wake, via suppression of the FB, which is thought as a sleep-induction center (Q. Liu et al., 2012; Ueno et al., 2012; Pimentel et al., 2016). In addition to these central neurons, peripheral neurons, such as ppk^+ neurons that project to the central brain, have been shown to have a role in the regulation of sleep homeostasis (Satterfield et al., 2022).

Many of these brain structures have been implicated in multi-behaviors. Like the MB and FB mentioned above, the EB has been shown to integrate sensory inputs to formulate locomotor

output commands, but our understanding of its role in sleep is still limited. In the present study, we identified subtypes of ring neurons that regulate sleep/structure by the following: (1) screening a small collection of EB drivers using thermogenetic activation; and (2) specifying the roles of several single subtypes in different sleep components using two models and intersection strategies. We found that R3m/R3p neurons contribute to daytime sleep, R4m neurons to wakefulness, and R3d neurons fragment sleep structure (Fig. 7F).

The role of these neurons in sleep may be intimately involved with their other functions. Previous studies found that R2, R3, R4d, and R4m subtypes appear to be tuned to visual stimuli (Shiozaki and Kazama, 2017; Fisher et al., 2019; Kim et al., 2019; Hardcastle et al., 2021). This sensory input may be an important cue to change sleep/wake status, and is likely influenced by the circadian system. Previous studies showed that the R5 subtype is linked to the control of sleep homeostasis and stabilization of sleep structure (S. Liu et al., 2016; C. Liu et al., 2019), and our analysis supports these findings. A recent study released on *bioRxiv* identified two subtypes: sleep-promoting R3m neurons and wake-promoting R3d neurons (Aleman et al., 2021). Consistently, we also observed that R3m contributes both sleep amount and sleep structure. 5HT7-GAL4⁺ neurons play an important role in sleep maintenance, when they are activated, sleep became fragmented (C. Liu et al., 2019). According to a recent anatomic analysis (Hulse et al., 2021), 5HT7-GAL4⁺ neurons include R3d, R3p, and R4d subtypes, and we narrowed the fragmentation effect down to a specific subtype (R3d) in the present study. However, more efforts are still needed to understand how a certain subtype of ring neuron responds to sensory inputs and how neuronal activity patterns form in the network. Future work examining the neural activity of each subtype of ring neurons that control distinct sleep components and the interaction with other behaviors may reveal fundamental information about the rules of the coding and integration of the brain.

References

- Aleman A, Omoto JJ, Singh P, Nguyen BC, Kandimalla P, Hartenstein V, Donlea JM (2021) Opposing subclasses of *Drosophila* ellipsoid body neurons promote and suppress sleep. *bioRxiv* 464469. <https://doi.org/10.1101/2021.10.19.464469>.
- Alpert MH, Gil H, Para A, Gallio M (2022) A thermometer circuit for hot temperature adjusts *Drosophila* behavior to persistent heat. *Curr Biol* 32:4079–4087.
- Artiushin G, Sehgal A (2017) The *Drosophila* circuitry of sleep-wake regulation. *Curr Opin Neurobiol* 44:243–250.
- Bausenwein B, Muller NR, Heisenberg M (1994) Behavior-dependent activity labeling in the central complex of *Drosophila* during controlled visual stimulation. *J Comp Neurol* 340:255–268.
- Bringmann H (2018) Sleep-active neurons: conserved motors of sleep. *Genetics* 208:1279–1289.
- Donlea JM, Pimentel D, Miesenbock G (2014) Neuronal machinery of sleep homeostasis in *Drosophila*. *Neuron* 81:1442.
- Fisher YE, Lu J, D'Alessandro I, Wilson RI (2019) Sensorimotor experience remaps visual input to a heading-direction network. *Nature* 576:121–125.
- Franconville R, Beron C, Jayaraman V (2018) Building a functional connectome of the *Drosophila* central complex. *Elife* 7:e37017.
- Hamada FN, Rosenzweig M, Kang K, Pulver SR, Ghezzi A, Jegla TJ, Garrity PA (2008) An internal thermal sensor controlling temperature preference in *Drosophila*. *Nature* 454:217–220.
- Hanesch U, Fischbach KF, Heisenberg M (1989) Neuronal architecture of the central complex in *Drosophila melanogaster*. *Cell Tissue Res* 257:343–366.
- Hardcastle BJ, Omoto JJ, Kandimalla P, Nguyen BM, Keles MF, Boyd NK, Hartenstein V, Frye MA (2021) A visual pathway for skylight polarization processing in *Drosophila*. *Elife* 10:e63225.
- Haynes PR, Christmann BL, Griffith LC (2015) A single pair of neurons links sleep to memory consolidation in *Drosophila melanogaster*. *Elife* 4:e03868.
- Herice C, Sakata S (2019) Pathway-dependent regulation of sleep dynamics in a network model of the sleep-wake cycle. *Front Neurosci* 13:1380.
- Hulse BK, Haberkern H, Franconville R, Turner-Evans DB, Takemura SY, Wolff T, Noorman M, Dreher M, Dan C, Parekh R, Hermundstad AM, Rubin GM, Jayaraman V (2021) A connectome of the *Drosophila* central complex reveals network motifs suitable for flexible navigation and context-dependent action selection. *Elife* 10:e66039.
- Isaacman-Beck J, Paik KC, Wienecke CF, Yang HH, Fisher YE, Wang IE, Ishida IG, Maimon G, Wilson RI, Clandinin TR (2020) SPARC enables genetic manipulation of precise proportions of cells. *Nat Neurosci* 23:1168–1175.
- Jin X, Tian Y, Zhang ZC, Gu P, Liu C, Han J (2021) A subset of DN1p neurons integrates thermosensory inputs to promote wakefulness via CNMa signaling. *Curr Biol* 31:2075–2087.e6.
- John B, Bellipady SS, Bhat SU (2016) Sleep promotion program for improving sleep behaviors in adolescents: a randomized controlled pilot study. *Scientifica (Cairo)* 2016:8013431.
- Joiner WJ, Crocker A, White BH, Sehgal A (2006) Sleep in *Drosophila* is regulated by adult mushroom bodies. *Nature* 441:757–760.
- Keene AC, Stratmann M, Keller A, Perrat PN, Vosshall LB, Waddell S (2004) Diverse odor-conditioned memories require uniquely timed dorsal paired medial neuron output. *Neuron* 44:521–533.
- Keene AC, Krashes MJ, Leung B, Bernard JA, Waddell S (2006) *Drosophila* dorsal paired medial neurons provide a general mechanism for memory consolidation. *Curr Biol* 16:1524–1530.
- Kim SS, Hermundstad AM, Romani S, Abbott LF, Jayaraman V (2019) Generation of stable heading representations in diverse visual scenes. *Nature* 576:126–131.
- Kottler B, Faville R, Bridi JC, Hirth F (2019) Inverse control of turning behavior by dopamine D1 receptor signaling in columnar and ring neurons of the central complex in *Drosophila*. *Curr Biol* 29:567–577.e566.
- Lebestky T, Chang JS, Dankert H, Zelnik L, Kim YC, Han KA, Wolf FW, Perona P, Anderson DJ (2009) Two different forms of arousal in *Drosophila* are oppositely regulated by the dopamine D1 receptor ortholog DopR via distinct neural circuits. *Neuron* 64:522–536.
- Lecompte D, Kaufman L, Rousseeuw P (1986) Hierarchical cluster analysis of emotional concerns and personality characteristics in a freshman population. *Acta Psychiatr Belg* 86:324–333.
- Lin CY, Chuang CC, Hua TE, Chen CC, Dickson BJ, Greenspan RJ, Chiang AS (2013) A comprehensive wiring diagram of the protocerebral bridge for visual information processing in the *Drosophila* brain. *Cell Rep* 3:1739–1753.
- Liu C, Meng Z, Wiggins TD, Yu J, Reed ML, Guo F, Zhang Y, Rosbash M, Griffith LC (2019) A serotonin-modulated circuit controls sleep architecture to regulate cognitive function independent of total sleep in *Drosophila*. *Curr Biol* 29:3635–3646.e3635.
- Liu D, Dan Y (2019) A motor theory of sleep-wake control: arousal-action circuit. *Annu Rev Neurosci* 42:27–46.
- Liu Q, Liu S, Kodama L, Driscoll MR, Wu MN (2012) Two dopaminergic neurons signal to the dorsal fan-shaped body to promote wakefulness in *Drosophila*. *Curr Biol* 22:2114–2123.
- Liu S, Liu Q, Tabuchi M, Wu MN (2016) Sleep drive is encoded by neural plastic changes in a dedicated circuit. *Cell* 165:1347–1360.
- Ofstad TA, Zuker CS, Reiser MB (2011) Visual place learning in *Drosophila melanogaster*. *Nature* 474:204–207.
- Omoto JJ, Nguyen BM, Kandimalla P, Lovick JK, Donlea JM, Hartenstein V (2018) Neuronal constituents and putative interactions within the *Drosophila* ellipsoid body neuropil. *Front Neural Circuits* 12:103.
- Parisky KM, Agosto Rivera JL, Donelson NC, Kotecha S, Griffith LC (2016) Reorganization of sleep by temperature in *Drosophila* requires light, the homeostat, and the circadian clock. *Curr Biol* 26:882–892.
- Pimentel D, Donlea JM, Talbot CB, Song SM, Thurston AJ, Miesenbock G (2016) Operation of a homeostatic sleep switch. *Nature* 536:333–337.
- Raccuglia D, Huang S, Ender A, Heim MM, Laber D, Suarez-Grimalt R, Liotta A, Sigrist SJ, Geiger JR, Oswald D (2019) Network-specific synchronization of electrical slow-wave oscillations regulates sleep drive in *Drosophila*. *Curr Biol* 29:3611–3621.e3613.
- Satterfield LK, De J, Wu M, Qiu T, Joiner WJ (2022) Inputs to the sleep homeostat originate outside the brain. *J Neurosci* 42:5695–5704.

- Scammell TE, Arrigoni E, Lipton JO (2017) Neural circuitry of wakefulness and sleep. *Neuron* 93:747–765.
- Seelig JD, Jayaraman V (2015) Neural dynamics for landmark orientation and angular path integration. *Nature* 521:186–191.
- Seidner G, Robinson JE, Wu M, Worden K, Masek P, Roberts SW, Keene AC, Joiner WJ (2015) Identification of neurons with a privileged role in sleep homeostasis in *Drosophila melanogaster*. *Curr Biol* 25:2928–2938.
- Shiozaki HM, Kazama H (2017) Parallel encoding of recent visual experience and self-motion during navigation in *Drosophila*. *Nat Neurosci* 20:1395–1403.
- Siegmund T, Korge G (2001) Innervation of the ring gland of *Drosophila melanogaster*. *J Comp Neurol* 431:481–491.
- Sitaraman D, Aso Y, Jin X, Chen N, Felix M, Rubin GM, Nitabach MN (2015) Propagation of homeostatic sleep signals by segregated synaptic microcircuits of the *Drosophila* mushroom body. *Curr Biol* 25:2915–2927.
- Ueno T, Tomita J, Tanimoto H, Endo K, Ito K, Kume S, Kume K (2012) Identification of a dopamine pathway that regulates sleep and arousal in *Drosophila*. *Nat Neurosci* 15:1516–1523.
- Wiggin TD, Goodwin PR, Donelson NC, Liu C, Trinh K, Sanyal S, Griffith LC (2020) Covert sleep-related biological processes are revealed by probabilistic analysis in *Drosophila*. *Proc Natl Acad Sci USA* 117:10024–10034.
- Young JM, Armstrong JD (2010) Building the central complex in *Drosophila*: the generation and development of distinct neural subsets. *J Comp Neurol* 518:1525–1541.
- Zhang Z, Li X, Guo J, Li Y, Guo A (2013) Two clusters of GABAergic ellipsoid body neurons modulate olfactory labile memory in *Drosophila*. *J Neurosci* 33:5175–5181.